

Decompressing Emulsion Droplets Favors Coalescence

Nicolas Bremond,* Abdou R. Thiam, and Jérôme Bibette

UPMC Univ. Paris 06, ESPCI, CNRS, 10 rue Vauquelin, 75005 Paris, France

(Received 19 September 2007; published 15 January 2008)

The destabilization process of an emulsion under flow is investigated in a microfluidic device. The experimental approach enables us to generate a periodic train of droplet pairs, and thus to isolate and analyze the basic step of the destabilization, namely, the coalescence of two droplets which collide. We demonstrate a counterintuitive phenomenon: coalescence occurs during the separation phase and not during the impact. Separation induces the formation of two facing nipples in the contact area that hastens the connection of the interfaces prior to fusion. Moreover, droplet pairs initially stabilized by surfactants can be destabilized by forcing the separation. Finally, we note that the fusion mechanism is responsible for a cascade of coalescence events in a compact system of droplets where the separation is driven by surface tension.

DOI: [10.1103/PhysRevLett.100.024501](https://doi.org/10.1103/PhysRevLett.100.024501)

PACS numbers: 47.55.df, 47.57.Bc, 47.61.Jd

Coalescence of two unstable liquid droplets is a complex phenomenon involving broad length and time scales. The complete scenario of such event is generally described as follows [1]: first the droplets approach each other, they get flattened as the pressure increases in the contact area, and then the thin interstitial film drains until the two interfaces interact via van der Waals forces that hasten the film draining and amplify thermal fluctuations of the interfaces that eventually merge leading to the coalescence of the two droplets. These fluctuations can be observed in a phase-separated colloids dispersion system [2], but are not accessible in our experiments. Here, we focus on the consequences of interface deformations generated by hydrodynamic forces involved in the coalescence process.

There are many industrial ways to produce emulsion and most of them rely on shearing [3]. It is known that depending on the volume ratio of the two phases as well as the viscosity ratio, shear could lead to coalescence and destruction of the emulsion [4]. Emulsification process is thus the place of a competition between breakup and coalescence where some of the hydrodynamic consequences are still unknown. However, an intensive work has already been made on the hydrodynamic interaction of two drops that collide in a flow generated by a four-roll mill device [5].

Most of the experiments dedicated to the study of emulsion stability are based on bulk measurements [3] where mean drop size and drop size distribution are monitored with low time resolution. This approach cannot explain fast and collective behaviors such as phase inversion occurring when a mechanical stress is applied on the emulsion. A clear description of the coalescence event at the level of a droplet pair is needed. We thus designed an experiment that enables us to isolate and monitor, with high space and time resolutions, the life of a large number of droplet pairs.

The experiments rest on microfluidics technology and, in particular, on the last developments of digital microfluidics that uses emulsion droplets as microreactors [6].

Indeed, it is possible to continuously create monodisperse emulsion droplets on chip [7] that can be handled in a network of microchannels [8]. A picture of the microfluidic device dedicated to the drop coalescence study is reported in Fig. 1. A train of water in oil droplets is generated by a flow-focusing module and then transformed into a train of droplet pairs after splitting. The use of a slightly asymmetrical loop allows to delay one droplet with respect to the other and thus to avoid the collision at the exit of the loop. Moreover, the distance between the two droplets can be adjusted prior to collision by removing part of the continuous phase. Finally, the collision is obtained by simply expanding the channel width. The devices are fabricated by soft lithography techniques [9]. We use the elastomer poly(dimethylsiloxane) (PDMS) (RTV 615, GE-Bayer Toshiba) for the replication of a resin mold with a height H of $22\ \mu\text{m}$. The reticulated polymer matrix is then bonded on a glass slide on the top of which a thin layer ($\sim 20\ \mu\text{m}$) of PDMS has been spincoated. The bonding is realized by a gradient of curing agent between the two layers [10]. Contrary to plasma-activated bonding, this protocol ensures that the channel walls become instantaneously hydrophobic, a necessary condition for the formation of water in oil emulsions without surfactants. The

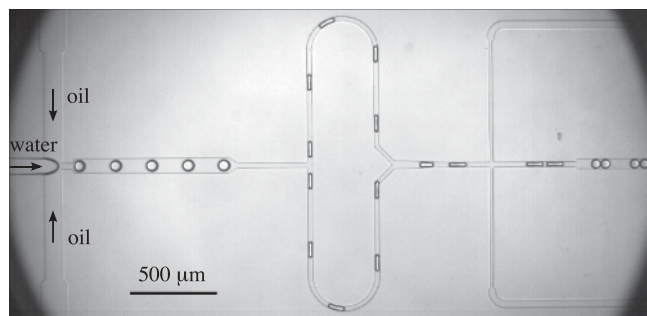


FIG. 1. Microfluidic device dedicated to the investigation of the coalescence of emulsion droplets.

dispersed phase is Milli-Q water and hexadecane (Sigma) is used as the continuous oil phase. Flows of both phases are driven by two syringe pumps (PHD 2200, Harvard Apparatus). Before proceeding to the first measurements and because hexadecane swells the PDMS, the newly made microfluidic circuits are rinsed with hexadecane until the channel width remain constant (this requires about half an hour of stabilization). The complete history of a droplet pair is recorded with a high speed camera (FASTCAM-X 1024, Photron) mounted on an inverted microscope (TE300, Nikon). Many thousands of coalescence events are recorded and automatically analyzed using image processing programs developed with MATLAB.

As depicted in Fig. 1, the channel width is initially narrower than the droplets size, forcing them to be elongated. The droplets collide when the channel suddenly expands. Droplets then relax to a circular shape but remain constrained in the transverse direction, which keeps them aligned and ensures the persistence of a plane of symmetry [Fig. 2(b)]. An example of the evolution of the distance D between the two centers of mass of the droplets versus the distance x is reported in Fig. 2(a) (solid circles). The origin of the x axis is chosen to the location where the channel width starts to increase. During the collision, D goes through a minimum and then increases as the droplets relax to a pancakelike shape. But, as shown in Fig. 2(d), D still increases after shape relaxation. Indeed, we find from image processing that the shape relaxation is achieved at $x \sim 80 \mu\text{m}$. Therefore, the further increase of D must be attributed to the oil flow. The dynamics of the separation

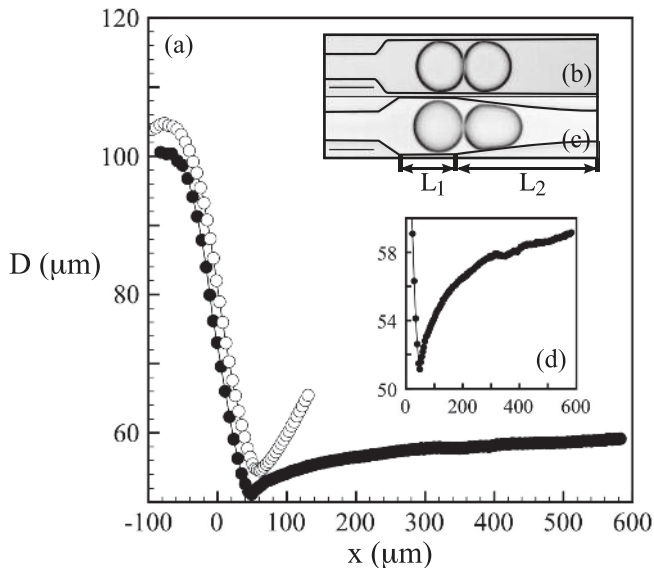


FIG. 2. (a) Evolution of the distance D between the two centers of mass of the droplets until they coalesce as a function of the distance x along the flow: ● without forcing (b) and ○ with a converging channel ($L_1 = 60 \mu\text{m}$, $L_2 = 200 \mu\text{m}$) (c). The scale bar in (b) and (c) is $50 \mu\text{m}$. (d) Close view of the trajectory $D(x)$ without forcing.

varies from pair to pair as a result of small and uncontrolled disturbance in the liquid flows. Moreover, small fluctuations of the droplet size may occur which also affect the separation process. As a consequence, the coalescence position x_c is distributed. Nevertheless, the main conclusion that arises from those observations is that the two droplets are always moving away from each other prior to coalescence.

Thanks to this observation, we designed microfluidic modules that enable us to force the separation and thus to trigger the destabilization of the droplet pairs. Figure 3 shows the time sequence of a droplet pair which passes through a symmetrical coalescence chamber. This sequence illustrates the main message of the paper: the separation of emulsion droplets favors coalescence. Indeed, the two initially elongated droplets collide because of the lateral expansion of the channel but do not coalesce. Then they relax to pancakelike shape and finally coalesce when the first droplet is aspirated in the converging part of the chamber. In order to control the separation, we designed an asymmetrical coalescence chamber having the geometry depicted in Fig. 2(c). An example of the evolution of the distance D between the two centers of mass is reported in Fig. 2(a) (open circles). As expected, the separation rate is more than 10 times faster than the situation without forcing.

When many pairs are processed through this asymmetrical chamber, we also observe that the location of coalescence x_c is distributed. In order to characterize this distribution, we plot in Fig. 4(a) the position x_c as a function of the parameter K which reflects the initial configuration of the pair. The parameter K is simply expressed as $K = WD_0/4R^2$, where D_0 is the distance between the centers of mass of the two elongated droplets

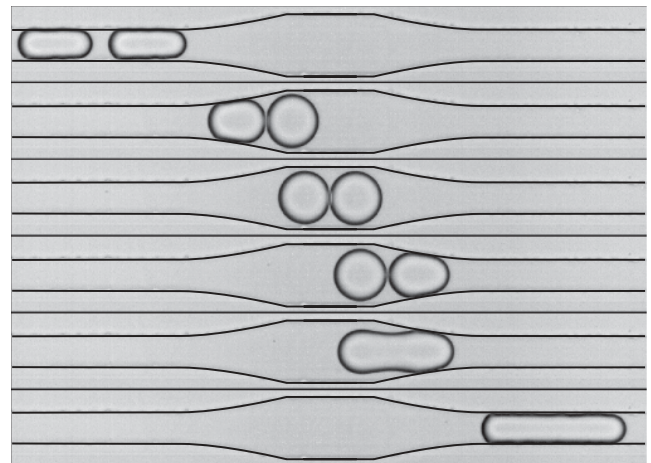


FIG. 3. Time sequence showing the destabilization of a droplet pair passing through a symmetrical coalescence chamber: collision, relaxation, separation, and fusion. The channel width expands from $36 \mu\text{m}$ to $72 \mu\text{m}$. From top to bottom, the time in milliseconds is 0, 3, 5, 7, 7.1, and 10.

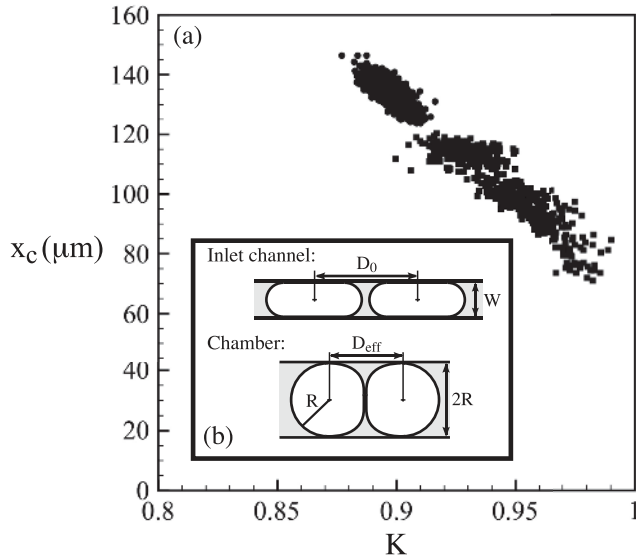


FIG. 4. (a) Correlation between the location of coalescence x_c and the parameter K when droplet pairs are passing through a converging channel ($L_1 = 60 \mu\text{m}$, $L_2 = 200 \mu\text{m}$) for two sets of flow rate conditions (units are $\mu\text{l/h}$: \bullet $q_o = 400$, $q_w = 100$ and \blacksquare $q_o = 200$, $q_w = 50$). (b) Definition of the parameter K that reflects the initial configuration of the pair ($K = D_{\text{eff}}/2R$ and reduces to $WD_0/4R^2$ by mass conservation).

right before entering the chamber, W the inlet channel width, and R the average radius of curvature of the two droplets within the chamber. The droplet deformation is therefore large for small K , and the collision is defined as gentle for K close to 1. Note that there is no chance that the droplets coalesce for K larger than 1. This parameter K can be readily obtained from a mass conservation argument as schemed in Fig. 4(b). For the two injection conditions reported in Fig. 4(a), black circles and black squares, the mean drop size R is respectively $28.5 \mu\text{m}$ and $29.5 \mu\text{m}$, and the initial distance D_0 is $94 \mu\text{m}$ and $105 \mu\text{m}$. The different values of K arise from small fluctuations, about 1%, of the parameters R and D_0 . From this plot it is clear that the whole process that leads to coalescence is strongly governed by the initial configuration of the pair.

Let us come back to the main question: what is the role of the droplet separation? A close view of the pair as it goes through the converging channel is shown in Fig. 5. The snapshot has been taken prior to coalescence that occurs 0.1 ms later. We observe the formation of two facing nipples in the contact area. We speculate that these nipples bring the two interfaces close enough until they merge. The formation of the nipples as the droplets are pulled apart is a consequence of their deformability. Contrary to the collision phase where the pressure increases between the drops with a maximum located along the axis of symmetry [1], the interstitial pressure drops down as they are being pulled apart. By symmetry, in the present situation, the pressure is minimum at the center of the interstitial film. This local

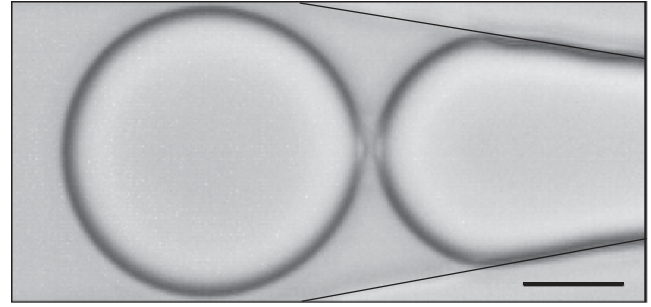


FIG. 5. Formation of two facing nipples in the contact area prior to coalescence induced by separating the droplets. The scale bar is $20 \mu\text{m}$.

low pressure induces the formation of a nipple. The scenario of nipple formation has been recently anticipated [11] but not observed. As far as we know, there is no model that describes this phenomenon.

Up to now, all the experiments were performed with clean interfaces. The next step is to see whether or not the forcing induces the coalescence of stabilized emulsion droplets. We therefore added 0.1% in mass of Span80 (Fluka) in hexadecane, a nonionic surfactant commonly used for stabilizing water in oil emulsions. The critical micellar concentration of Span80 in hexadecane is around $2 \times 10^{-2} \text{ mM}$ for a water/hexadecane system and, at this concentration, a molecule occupies an area of about 35 \AA^2 [12]. The actual concentration is thus nearly 10^2 times larger than the critical micellar concentration. To be more precise, for a droplet radius of $30 \mu\text{m}$ and a flow rate ratio q_o/q_w equal to 4, the remaining surfactant concentration c^0 within the continuous phase is still 10 times larger than the concentration needed for fully covering the droplet surface. We first notice that surfactants prevent coalescence when the separation is not forced. On the other hand and despite the saturation of interface by surfactants, droplet pairs are destabilized when they flow through the fusion chamber. This phenomenon is interpreted to be the result of a local depletion of surfactant molecules at the interface during the nipple formation as the interface area suddenly increases. Indeed, the characteristic time of the interface deformation is of the order of 1 ms, which remains shorter than the characteristic time τ_D required for surfactant molecules to adsorb (for the present concentration D is about $7 \times 10^{-11} \text{ m}^2/\text{s}$ [13] and therefore $\tau_D = (\Gamma^0/c^0)^2/D \sim 10 \text{ s}$ [14], where Γ^0 is the equilibrium adsorption). We stress that the adsorption time is based on a diffusion scenario and does not take into account a possible convection of surfactants from the flow in the interstitial film, a regime that is predominant during the emulsification step.

We now consider the effect of this mechanism at the level of a collection of densely packed droplets. The destabilization of a compact one-dimensional train of emulsion droplets which are free of surfactants is shown in

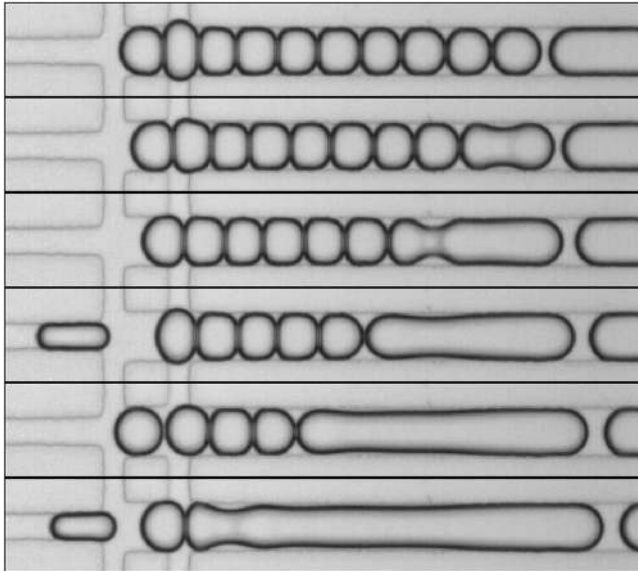


FIG. 6. Time sequence of the cascade of coalescence initiated in a compact train of droplets. The time step between two frames is 1 ms; the main channel width is 65 μm .

Fig. 6. We observe that the fusion of a pair located at one side of the compact train triggers the coalescence of neighboring droplets. Because of the minimization of surface energy, the interfaces between the second and the third droplets move away from each other when the first two droplets coalesce. We speculate that the separation, which is now driven by surface tension, induces the formation of two facing nipples (Fig. 5) that destabilizes the pair formed with the next droplet. This scenario is repeated and a cascade of coalescence is initiated.

We have reported an investigation of the destabilization process of an emulsion under flow with the help of a microfluidics device. The coalescence event is monitored at the level of a droplet pair. We demonstrate a counter-intuitive phenomenon when the two droplets collide: coalescence occurs during the separation phase and not during the impact. Separation induces the formation of two facing nipples in the contact area that hastens the connection of the interfaces prior to fusion. Moreover, droplet pairs initially stabilized by surfactants can be destabilized by forcing the separation. Finally, we note that the fusion mechanism is responsible for a cascade of coalescence events in a compact system of droplets where the separation is driven by surface tension. To conclude, we hypothesize that this destabilization mechanism may ex-

plain a variety of empirical observations reported about coalescence under shear in concentrated emulsions. It is indeed very often observed that in a dense system submitted to shear very large drops can form within a background of much smaller ones [3], as would cause an heterogeneous coalescence process. This effect has been, namely, attributed to the possible role of some dirt particles [15]. Here, we show that hydrodynamics can also cause a cascade of coalescence events in good agreement with the observation of the growth of a limited number of large drops. Finally, we also think that some type of phase inversion phenomena that are shear induced could arise from this cascade of coalescence events.

The authors acknowledge Jean Baudry and Elise Lorenceau for stimulating discussions and Hervé Willaime for his help in microfabrication. This work was supported by the European Network MiFem under Contract No. 028417.

*Nicolas.Bremond@espci.fr

- [1] A. K. Chesters, *Chem. Eng. Res. Des.* **69**, 259 (1991).
- [2] D. G. A. L. Aarts, M. Schmidt, and H. N. W. Lekkerkerker, *Science* **304**, 847 (2004).
- [3] F. Leal-Calderon, V. Schmitt, and J. Bibette, *Emulsion Science—Basic Principles* (Springer, New York, 2007).
- [4] K. Meleson, S. Graves, and T. G. Mason, *Soft Mater.* **2**, 109 (2004).
- [5] L. G. Leal, *Phys. Fluids* **16**, 1833 (2004).
- [6] H. Song, J. D. Tice, and R. F. Ismagilov, *Angew. Chem., Int. Ed. Engl.* **42**, 768 (2003).
- [7] S. L. Anna, N. Bontoux, and H. A. Stone, *Appl. Phys. Lett.* **82**, 364 (2003).
- [8] D. R. Link, S. L. Anna, D. A. Weitz, and H. A. Stone, *Phys. Rev. Lett.* **92**, 054503 (2004).
- [9] J. C. McDonald, D. C. Duffy, J. R. Anderson, D. T. Chiu, H. K. Wu, O. J. A. Schueller, and G. M. Whitesides, *Electrophoresis* **21**, 27 (2000).
- [10] M. A. Unger, H. P. Chou, T. Thorsen, A. Scherer, and S. R. Quake, *Science* **288**, 113 (2000).
- [11] Y. Yoon, M. Borrell, C. C. Park, and L. G. Leal, *J. Fluid Mech.* **525**, 355 (2005).
- [12] L. Peltonen, J. Hirvonen, and J. Yliruusi, *J. Colloid Interface Sci.* **240**, 272 (2001).
- [13] J. R. Campanelli and X. H. Wang, *J. Colloid Interface Sci.* **213**, 340 (1999).
- [14] F. Ravera, M. Ferrari, and L. Liggieri, *Adv. Colloid Interface Sci.* **88**, 129 (2000).
- [15] P. G. de Gennes, *Chem. Eng. Sci.* **56**, 5449 (2001).